FIELD OBSERVATIONS OF RIPPLE AND MEGARIPPLE DYNAMICS IN THE NEARSHORE

Jon Miles[1], Anthony Thorpe[1], Paul Russell[1] and Gerd Masselink[1]

Abstract

Field measurements of megaripples and wave ripples were made in the surf and shoaling zones of a sandy macrotidal dissipative beach at Perranporth, England, in water depths up to 6 m, and wave heights up to 1.1 m. Megaripple heights were largest when orbital velocities were in the range 0.25 to 0.4 m/s, and reduced in height with increases in mean current speed. Wave ripples co-existed with megaripples and contributed up to 12% of the seabed elevation variance. Wave ripples heights increased with decreasing orbital velocity but reduced in height when mean currents were strong. Wave ripple and megaripple migration was generally onshore-directed in deeper water, and increased with incident wave skewness in shallower water. Onshore migration was reduced to zero when the offshore-directed mean flow was greater than 0.15 m/s.

Keywords: surf zone, ripples, megaripples, ripple migration rates, sonar ripple profiler, field measurements.

1. Introduction

In sandy beach environments, ripples on the seabed develop in a variety of conditions, and have characteristics that depend on the forcing hydrodynamics and sediment size. In wave dominated conditions, ripples may develop with a typical wavelength of ~0.2 m (Nielsen, 1992). Larger features known as megaripples develop in energetic conditions in the surf zone, with typical wavelengths of ~1 m (Gallagher et al., 1998). Previous field measurements indicate that wave ripples and megaripples exist in different locations in the nearshore zone (Thornton et al., 1998), and migration rates depend on their cross-shore location (Masselink et al., 2007), on wave skewness (Crawford and Hay, 2001) and wave asymmetry (Gallagher et al., 1998). New field observations in this paper suggest that there are times when both megaripples and wave ripples co-exist in the beach environment, and that they may migrate at different rates. Detailed measurements of bedform sizes and migration rates are presented from a sandy dissipative beach in North Cornwall (UK) from a variety of conditions.

2. Review

In a unidirectional flow, current-forced bedforms evolve as shear stress increases, through a sequence of: low stage flat bed ripples, to dunes, then an upper stage plane bed, and finally antidunes (Dyer 1986, Neilsen, 1992). Ripples in unidirectional flows typically scale with a length of 0.2 m and height 0.06 m, (Allen 1968). Yalin (1964) parameterized ripple length from the grain size ($\lambda = 1000$ D), and ripple height $\eta = \lambda/7$. As the shear stress increases, current-dunes develop, with typical wavelengths of 0.6 to 30 m, and heights 0.06 to 1.5 m. Dune length is governed by water depth ($\lambda = 2\ \pi$ h), and dune height scales to maximum of (h/6) (Yalin, 1964). In high flows and shallow depths, bedforms may migrate against the flow direction, in which case they are known as antidunes.

[1]School of Marine Science and Engineering, Plymouth University, Devon, PL4 8AA, UK.

Wave ripples are typically symmetrical in shape (Masselink and Hughes, 2003) and have been shown to migrate onshore due to wave asymmetry (Fredsoe and Diegard, 1992). Wave ripple heights typically increase with orbital excursion, and wavelengths increase with ripple heights (Nielsen, 1992). In energetic conditions in the surf zone, features larger than wave ripples may develop and these are known as megaripples. These have heights in the range η = 0.1 to 1 m, and lengths λ = 0.5 m to 5 m, (Gallagher et al., 1998; Gallagher, 2003). Megaripples are three dimensional, and although they may take on a regular alongshore structure, they may also develop as hummocks and holes in a less regular distribution (Gallagher, 2003).

Blondeaux et al. (2000) identified that in conditions with both waves and currents, the bed may display features of both wave and current ripples or other bedforms. Dyer (1986) identified that in a combined flow, one bedform will be superimposed on another. Bagnold (1963) classified ripples as either: sharp crested vortex ripples (calm conditions), with η / λ = 0.15; post-vortex ripples with η / λ = 0 to 0.15, or plane bed conditions, where shear stresses are above a threshold value.

Gallagher et al. (1998) and Gallagher (2003) measured temporal and spatial distributions of ripples in the nearshore over a 6 week period with wave heights in the range 0.1 to 4 m. The bedforms were in the size range η = 0.1 to 1 m, and had wavelengths λ = 0.5 m to 5 m. Megaripples were present 60% of the time. Onshore migration of megaripples was found to be related to wave asymmetry. The net ripple migration direction was found to result from a combination of the wave and current flows and directions (Gallagher, 2003). Thornton et al. (1998) observed bedforms from a large range of conditions at Duck94. Mild waves & weak currents led to wave ripples. Storm waves and strong longshore currents led to megaripples in the trough. Megaripples were observed in a rip channel. Newly formed wave ripples were found to co-exist with residual bedforms, creating complex patterns of topography. Masselink et al. (2007) found variations in ripple migration rates across the surf zone on a relatively coarse grained beach (D50 = 0.69 mm) at Sennen, UK. Ripple heights of 0.05 m and lengths of 0.35 m were recorded. Migration rates varied from 0.1 cm/min onshore in the shoaling zone, to 2 cm/min and onshore in the outer surf, and no transport in the inner surf.

The migration rate of ripples has been suggested to depend on mobility number (Vincent and Osborne, 1993; Traykocski et al. 1999). The direction of transport may follow the wave skewness (Crawford and Hay, 2001) or the wave asymmetry (Gallagher et al., 1998). Doucette (2002) made visual observations of ripple migration on a coarse sandy beach (D50 = 0.70 mm). The beach was sea breeze dominated, and ripples with heights of 0.05-0.15 m and lengths of 0.3 to 1.2 m were found to migrate onshore at rates of up to 0.2 cm/min. In strong currents such as feeder currents and rip currents, Sherman et al. (1993) found that lunate megaripples migrated in the same direction as the mean current. In a flow of 0.4 to 0.6 m/s in 0.71 m depth and wave height 0.65 m (T = 10.6 s), with D50 = 0.33 mm, ripples of length 1.6 m and height 0.16 m migrated at 1.65 cm/min.

3. Field measurements

Field measurements were made at a high energy, macrotidal dissipative sandy beach at Perranporth (North Cornwall, UK) (Figures 1 & 2). Perranporth has a mean tidal range of 6.1 m, and a mean offshore wave height of 1.6 m (Davidson et al., 1997). Sediments at the site were medium sand (D50 = 0.28 mm). Two separate field deployments were carried out in May 2011 and October 2011, each gaining data for six separate high tides. Tides are identified here as 11-16 and 21-26 respectively. Measurements were made by deploying a rig of instruments near the low water mark, and instruments

logged data as the tide flooded and ebbed over the rig. This allowed measurements to be made in a variety of water depths from 1 to 6 m, and in a variety of conditions in the surf and shoaling zones.

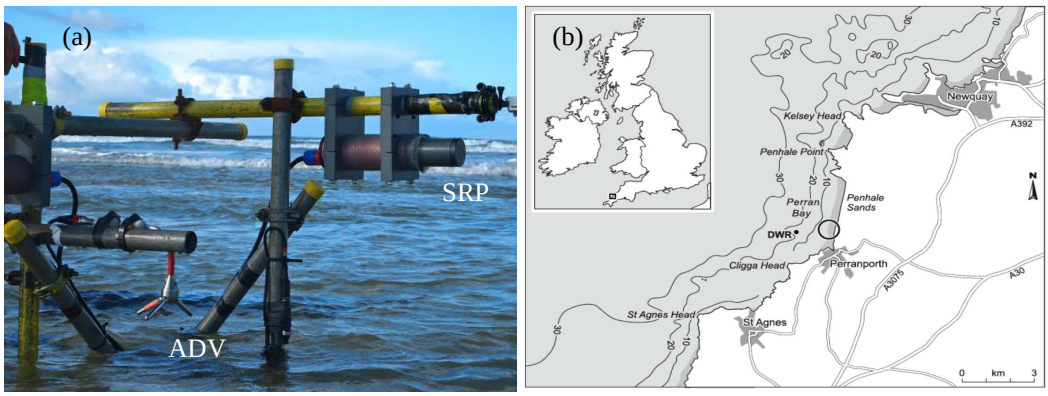

Figure 1: (a) Photo of instruments deployed showing the Sonar Ripple Profiler (SRP) and Acoustic Doppler Velocity meter (ADV); (b) The deployment location at Perranporth is indicated (circle).

Flow velocities were measured using an Acoustic Doppler Velocity Meter (ADV), with a sensing volume 25 cm above the bed. Mean water depths and wave heights were measured using a pressure transducer, deployed at bed level. Hydrodynamic data were recorded at 16 Hz or 8 Hz, depending on the specific tide. A Sonar Ripple Profiler (SRP) measured a line scan of seafloor elevation. The SRP was positioned 90 cm above the bed, and measured a 2 m on-offshore line once per minute. Data was post-processed to give regular horizontal (on-offshore) spacing between points of ~1 cm over the 2 m footprint of the scanner.

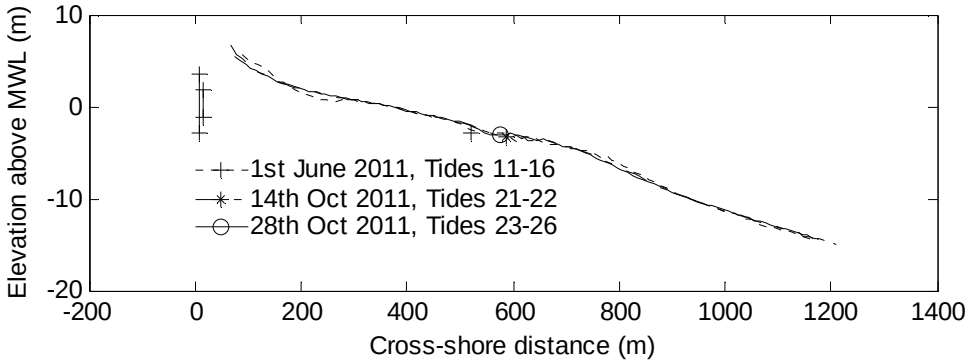

Figure 2: Beach profiles for the experiment period, showing the rig positions. Vertical bars show the range of spring and neap tides. Instrument rig locations are identified for the different tides.

4. Hydrodynamics overview

Data from the ADV and Pressure transducer were divided into 10-minute runs for processing (Figure 3). Data logging for the first 6 tides was only possible for a narrow time window around high tide

when there was sufficient water depth for the SRP. During the second set of 6 tides, data was collected in a larger range of water depths. Data here is clipped at the start of the flood and the end of the ebb to only show hydrodynamic data for runs when bedform data from the SRP is available. This is limited to depths greater than 1 m, when the water completely covered the SRP.

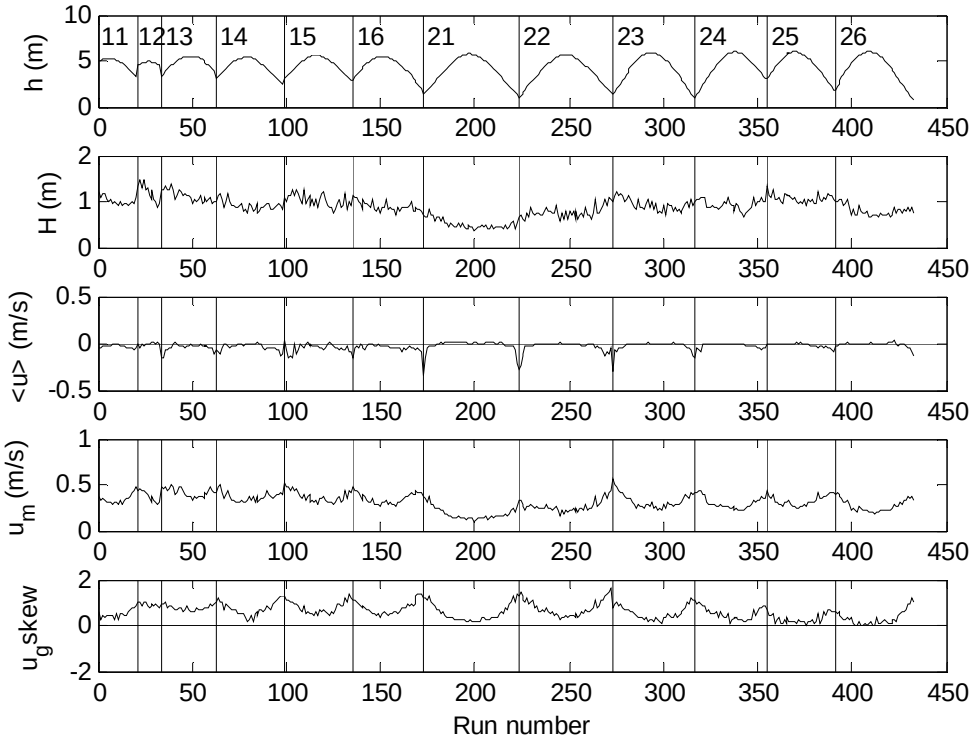

Figure 3: Hydrodymamic data, showing water depth (h), wave height (H), mean flows (<u>), orbital velocities (u_m), velocity skewness (u_g skew) calculated for 10-minute sections of data.

Wave heights ($H_{1/3}$) calculated at high tide for each of the tides recorded were in the range H = 0.49 m to 1.14 m. The corresponding breakpoint wave heights were 0.54 m to 1.46 m. Wave periods (not shown) indicated mostly swell waves for the measured tides, with period in the region 9.5 to 10.9 s, although data was also collected for wave period 7.7s (tides 25 and 26).

Mean flows at the ADV were either close to zero at high tide, or offshore directed in shallower water (in the surf zone) at either side of high tide. Mean flows reached a maximum (offshore directed) strength of -0.34 m/s. Velocity variances (not shown) also peaked in the shallow water at the start and end of the tide, but were modulated by the offshore wave height. Infragravity variance was generally small at high tide (2%), but increased in the shallower water in the surf zone. The maximum infragravity contribution was 17.6% of the total velocity variance (run 224, coinciding with the maximum offshore-directed mean flow). On other tides, the typical maximum infragravity contribution was in the range 8% to 12% at low tide.

Orbital velocities generally increased on days when the wave heights were larger, and also increased when the water depth over the rig was shallower. A similar pattern was followed by the orbital excursion. Incident wave velocity skewness and asymmetry were calculated following the approach

of Elgar et al. (1998). Wave skewness increased in a more pronounced manner than the orbital velocity in shallow water, reaching a maximum of 1.6 at run 272. Wave asymmetry (not shown) did not follow a clear pattern in the initial six tides, and was small (and negative) in the second set of 6 tides, with a magnitude of approximately -0.15. Consistent with previous measurements, (Miles, 2013), wave asymmetry became positive (onshore-directed) in water shallower than the SRP data presented here, reaching a maximum of 0.48 in 0.43 m water depth (tide 21).

5. Bedforms analysis

Initial investigations of SRP data from high tide in tide 21 showed short wave ripples developed on the crests of a megaripple (Figure 4). Wave heights were ~0.5 m, wave period 9.5 s, and mean currents were weak (<0.1 m/s). Spectral analysis of the bed surface elevation data showed a trough at 0.35 m wavelength, and this value was used in the subsequent analysis to separate wave ripples (typical $\lambda \sim 0.2$ m) from megaripples (typical $\lambda \sim 1$ m) using a frequency domain low/high pass filter.

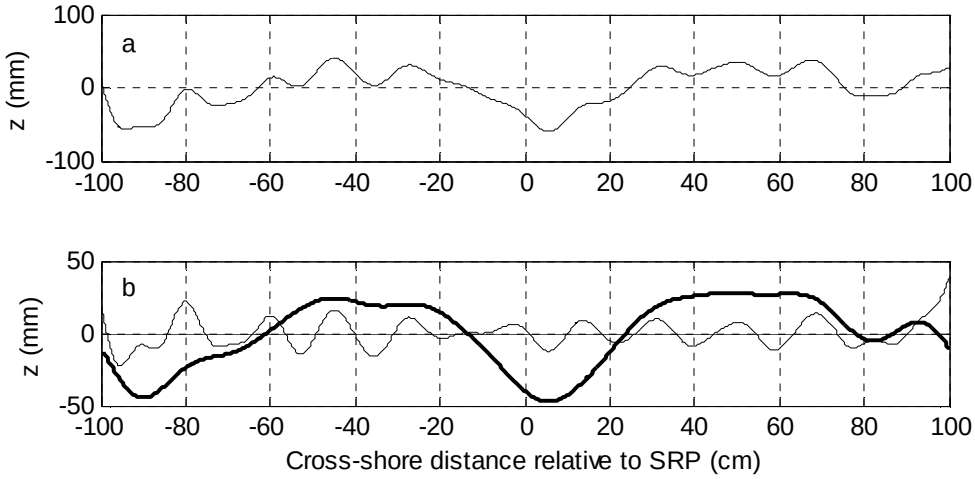

Figure 4: Measured bed elevation (a), and filtered wave ripple and megaripple components of bed elevation (b).

From each tide of data, consecutive linescans of bed elevation were time-stacked in order to visualize the bedform processes associated with that tide. Two tides of data are shown here (Figure 5) to indicate the differences observed from small waves (tide 21 with H = 0.49 m) to larger waves (tide 22 with H = 0.75 m). An obvious difference in the two plots is the complex bedform structure that appears in tide 21. There appears to be an underlying megaripple structure of length ~1.2 m. In deeper water, (run 190 onwards) a shorter wavelength set of ripples develops on the crest of the megaripple, with wavelength ~ 20 cm. The development of the shorter ripples does not appear to happen in the second tide, when waves are larger. In the small wave conditions in tide 21, the megaripple initially migrates shoreward, then stabilizes, before migrating shoreward again towards the end of the tide. In the final part of the data, it migrates offshore. When moving, the shorter wave ripples appear to migrate shoreward on one of the two megaripple crests. They reduce in size as the water gets shallower and as the megaripple starts to migrate shoreward. In the larger wave conditions, the megaripple appears to migrate shoreward for most of the tide, although the bed appears to flatten off in the shallowest water (after run 270).

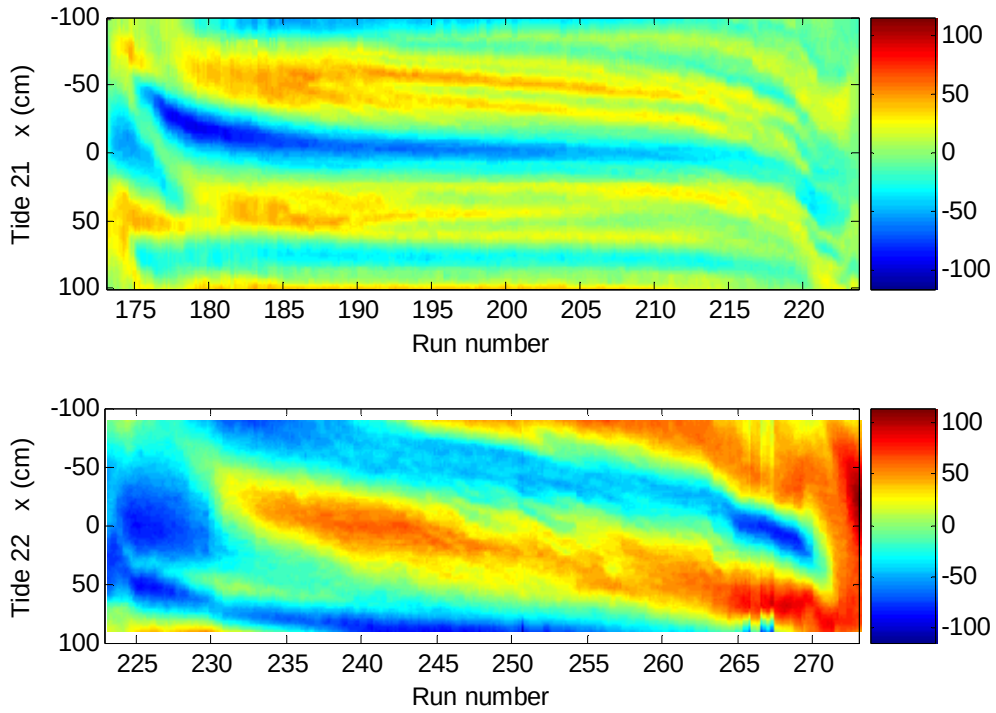

Figure 5: Time-stacked linescans of surface elevation (mm) for tide 21 (H = 0.49 m) and tide 22 (H = 0.79 m). Cross-shore distance (x) is shown as +ve shoreward (i.e. migration direction is mostly shoreward).

6. Bedform variation

In order to quantify the observations across the whole dataset, and examine the relationships with the hydrodynamic parameters, bedform parameters representing 10-minute sections of SRP data corresponding to the hydrodynamic parameters were calculated. Each SRP line scan was decomposed into a wave ripple component ($\lambda < 35$ cm) and a megaripple component ($\lambda > 35$ cm) using a frequency domain filter. The line scans (raw, wave ripple, megaripple) of bed elevation were then analysed to quantify bedform height, using the approach of Masselink et al. (2007). Migration rate of the bedforms was calculated from the cross-correlation between scans separated by a 5-minute time interval (following Masselink et al., 2007). Averaged bedform parameters for runs of 10 consecutive line scans were then calculated (Figure 6).

Megaripple heights were generally in the order of 10 - 20 cm, whereas wave ripple heights were generally of height 1-2 cm. Wave ripples became most prevalent when wave conditions were small. Megaripples appeared to reduce in size towards the start and end of the tide (in shallower water), co-incidental with the increase in orbital velocity. Wave ripples appeared to develop when the wave heights were at their smallest (runs 200, 420), but favoured deeper water for their development. The relative contribution of wave ripples can be expressed as the ratio of bed elevation variance in the filtered wave ripple data against the variance of the unfiltered bed data (parameter F_{wr}). The wave ripples contribution was up to 12.3% of the total variance.

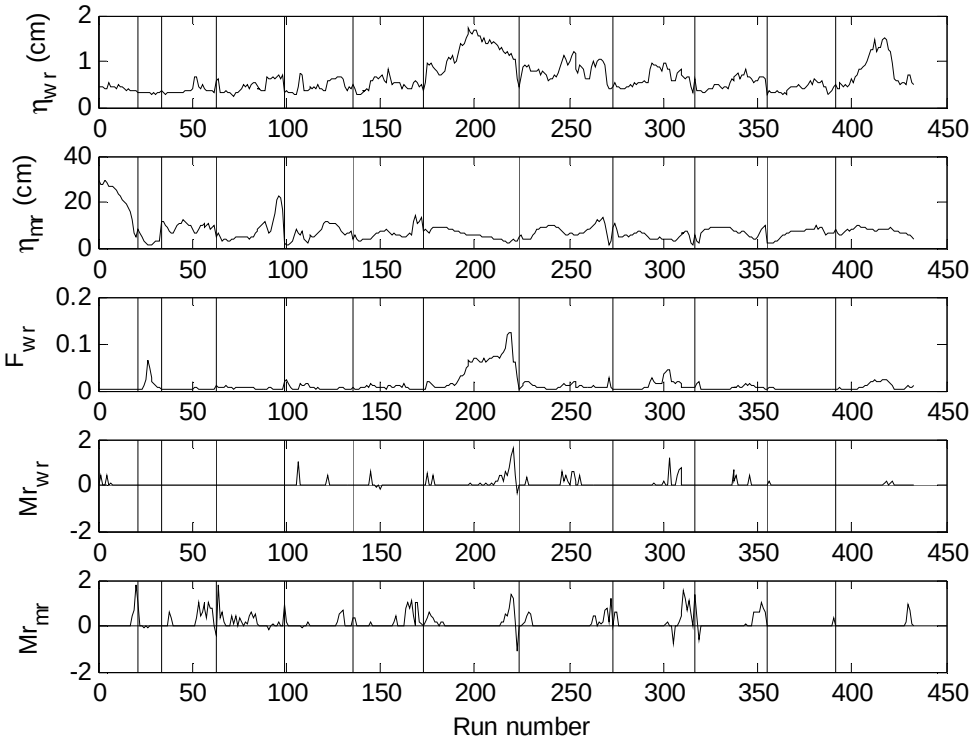

Figure 6: Bedform parameters, showing wave ripple height (η_{wr}), megaripple height (η_{mr}), ratio of wave ripple variance to un-filtered bed elevation variance (F_{wr}), wave ripple migration rate (Mr_{wr}) and megaripple migration rate (Mr_{mr}). Units of Mr are cm/min.

Megaripple and wave ripple migration was found to be predominantly onshore, and up to 1.9 cm/min. The movement of both wave ripples and megaripples did not form a clear pattern through the tide. There is some evidence that the megaripples migrated most quickly at the beginning or end of the tide, when the wave skewness was largest. The direction of migration of the megaripples was mainly onshore, in the direction of the wave skewness. At the end of tide 21, the megaripples turned offshore, and this may be due to the increasing influence of the mean offshore flow. In other tides in the second set of 6 experiments, the rate of migration also reduced when the instruments were in shallower water, and experiencing stronger offshore-directed mean flows, suggesting that the wave skewness and mean flow compete to control the direction of migration of the megaripples. Wave ripples also migrated predominantly onshore. In tide 21 when they were most prominent, they followed a similar migration trend to the megaripples, but were flattened in the more energetic conditions in shallow water.

7. Ripple development

The conditions for the development of megaripples and wave ripples were examined (Figure 7 & 8). Wave ripple heights were maximum when mean currents were zero, (Figure 7, top left panel). Wave ripples increased in height with reducing incident wave orbital velocity. There is some evidence that the ripple height increased with water depth, however this is complicated by the variation in orbital velocities due to varying incident wave conditions.

Megaripples were at their maximum height when mean velocities were offshore (~0.05 m/s). The largest megaripples developed when the orbital velocity was in the range 0.25 to 0.4 m/s, from a measured range of 0.1 to 0.57 m/s. Megaripple size was weakly linked to water depth, with some evidence that the larger megaripples occur in deeper water.

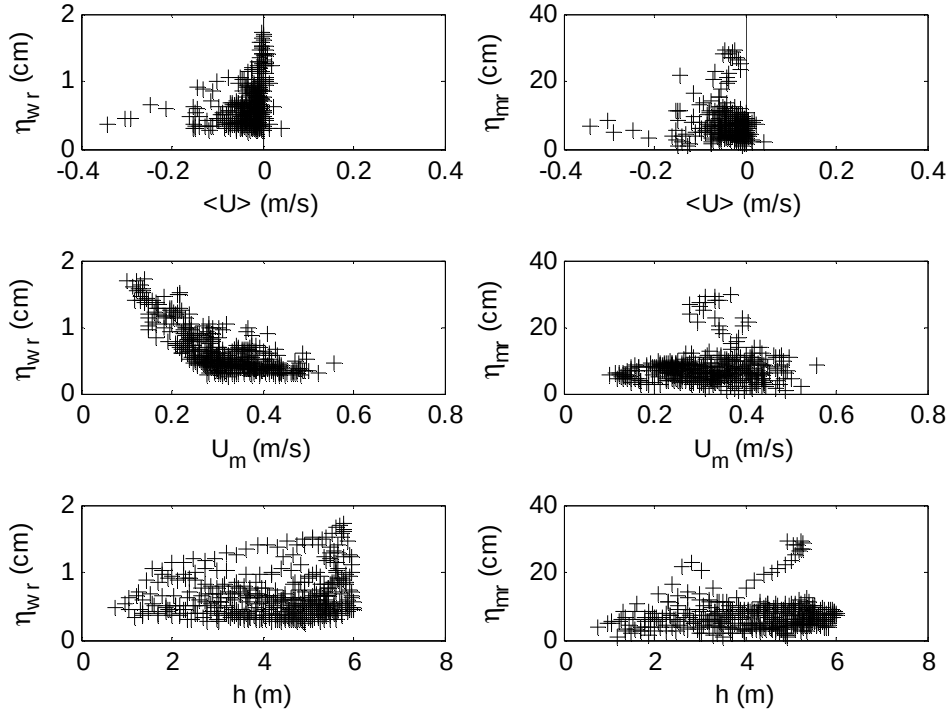

Figure 7: Height (η) of wave ripples (wr) and megaripples (mr) against mean velocity (<U>), orbital velocity (U_m) and water depth (h).

8. Migration rates

The time series in Figure 6 suggest that wave ripple migration rates were generally larger in shallower water, however this in itself is not a forcing parameter for migration. Wave ripples and megaripples both migrated at their maximum speeds when the incident wave skewness was large (Figure 9 & 10). Large negative (offshore-directed) flow velocities appeared to reduce the migration rate to zero, or turn it offshore in one case (Figure 9, top panel). The onshore wave ripple migration is maximum when the wave skewness is large and directed onshore, which corresponds to the time when offshore flow is approximately 0 to 0.1 m/s, (Figure 10 top panel). Mean flows greater in magnitude than -0.1 m/s and -0.16 m/s appear to coincide with migration rates reducing to zero for wave ripples and megaripples respectively, (Figure 10). Wave ripples and megaripple migration rates were not well correlated with wave asymmetry in the deeper water data, (Figure 9, bottom panel).

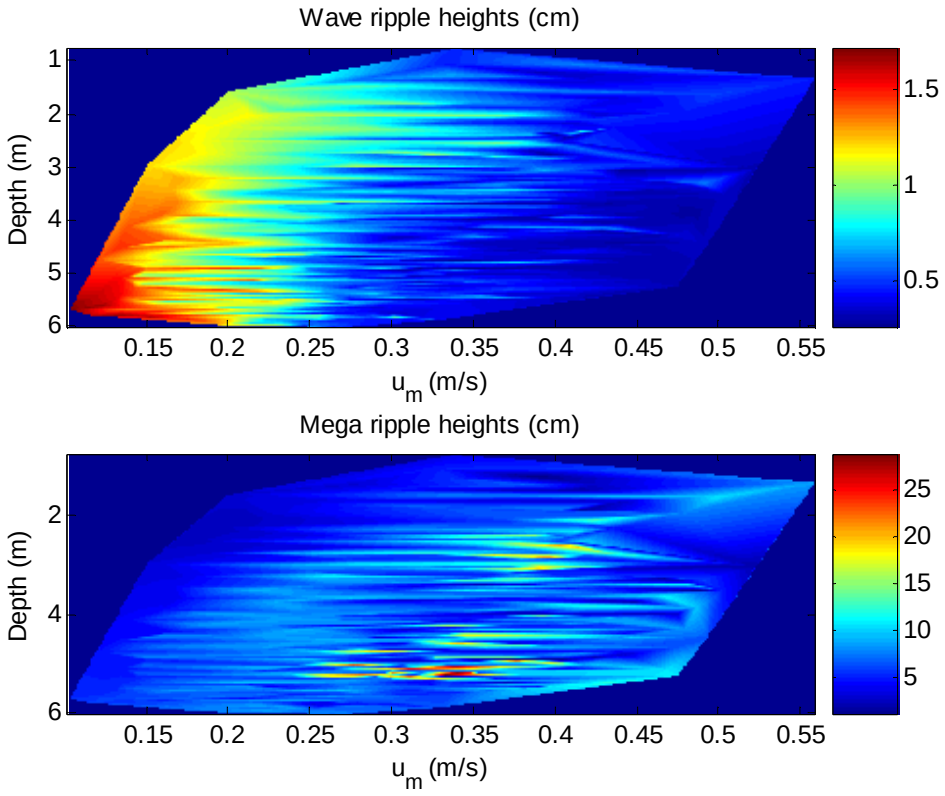

Figure 8: Heights of wave ripples and megaripples illustrated as a function of depth (m) and orbital velocity (u_m).

9. Discussion

Instruments on the rig in this experiment were located near the low water mark, in a shallow trough where it was possible to see the bedforms at low tide. This gives confidence in the presentation of megaripple data from the SRP. Supporting the data, observations by divers indicated that the megaripples persisted as the water depth increased, and that they covered an extensive alongshore and cross-shore area. In the second six tides of data, the trough also experienced rip current conditions when the water was shallow (~1 m) (Thorpe et al., 2013), and this increased the offshore directed mean flow component in the velocity data. This possibly contributes to the offshore-directed migration at the end of tide 21. The frequency and intensity of rip flows reduced as the water depth increased.

The wave ripples in this data are in the length range indicated by Yalin (1964) for current ripples, with $\lambda = 1000$ D giving a length of 28 cm, and a height of $\eta = \lambda / 7 = 4$ cm. However, their size reduced as the current and associated shear stress increased, and their height increased with orbital excursion, as indicated by Nielsen (1992) for wave generated ripples. The height of the wave ripples (1-2 cm), and their length of 20 cm, gives them a characteristic steepness of 0.05 to 0.1. They are therefore likely to be 'post-vortex' wave ripples, in Bagnold's (1963) classification. The megaripples ($\lambda > 35$ cm) have length scales and heights that tie in with Gallagher et al.'s (1998) classification for 'megaripples', and these exist in combined wave and current environments. Although they may have features similar to dunes (Yalin, 1964) in the shallowest water levels measured, (i.e. their height (~20 cm) is appropriate

for the water depth when the depth is 1.2 m), their height reduces with increasing current (shear stress), and so they are unlikely to be current dunes.

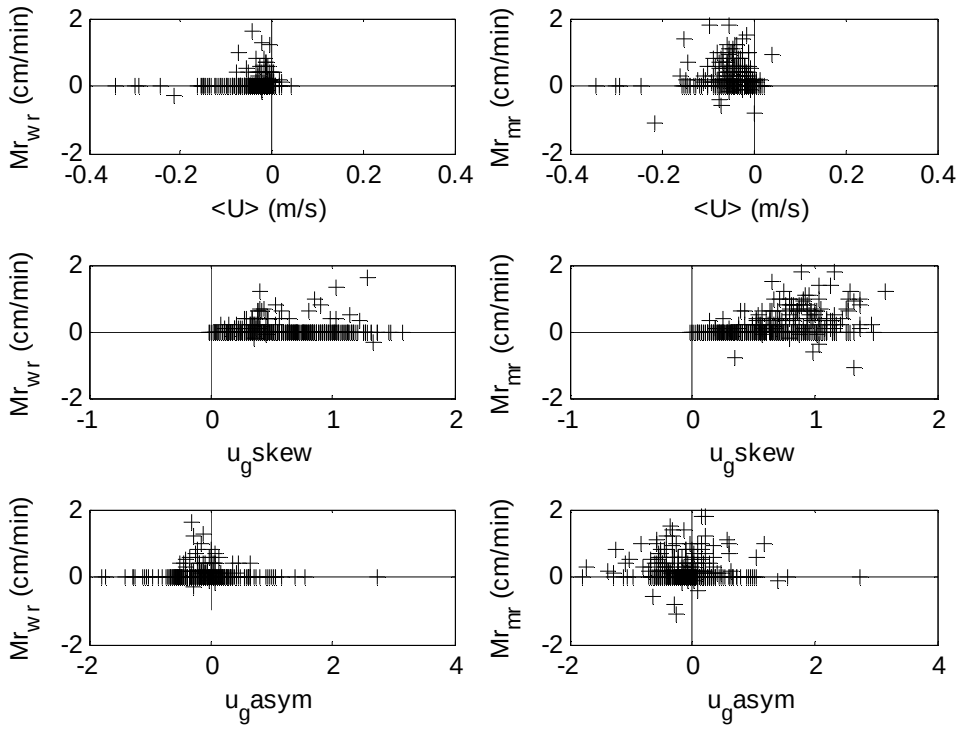

Figure 9: Migration rate (Mr) of wave ripples (wr) and megaripples (mr) against mean velocity (<U>), incident wave velocity skewness ($u_g$skew) and incident wave asymmetry ($u_g$asym).

Both megaripples and wave ripples migrated shoreward (c.f. Doucette, 2002), and generally moved in the direction of wave skewness, similar to Crawford and Hay (2001). Masselink et al. (2007) also documented an onshore migration direction, and a reduction in migration rates in the deeper water in the shoaling zone, compared to the outer surf zone. Like Masselink et al.'s (2007) data from the inner surf zone, the migration rates reduced in shallow water in this paper, and in this case this happened when the offshore-directed flow increased. This offshore-directed flow may be due to undertow (c.f. Masselink and Black, 1995) or may be the outer part of an intermittent rip current in the shallower water (Thorpe et al., 2013). Sherman et al's (1993) data also indicates that in conditions where the flow strength is strong, the balance may be in favour of the mean flow (i.e. offshore).

Although wave asymmetry is considered to be a driver of onshore bedform migration (Gallagher et al., 1998; Fredsoe and Diegard, 1992), in this case the wave asymmetry values were small when the SRP was submerged, and wave asymmetry was therefore unlikely to bring about the observed shoreward movement of the bedforms. Positive (onshore-directed) wave asymmetry was identified for water depths < 1 m in this data, but bedform observations were not possible in these shallow depths because the SRP required at least 1 m of water in order to gain a reasonable scan length. In the shallow water it is possible that the megaripple migration would have been forced onshore by wave asymmetry, but asymmetry would compete against the offshore flow by the mean current, and also against the flattening effect of higher orbital velocities in the inner-surf zone.

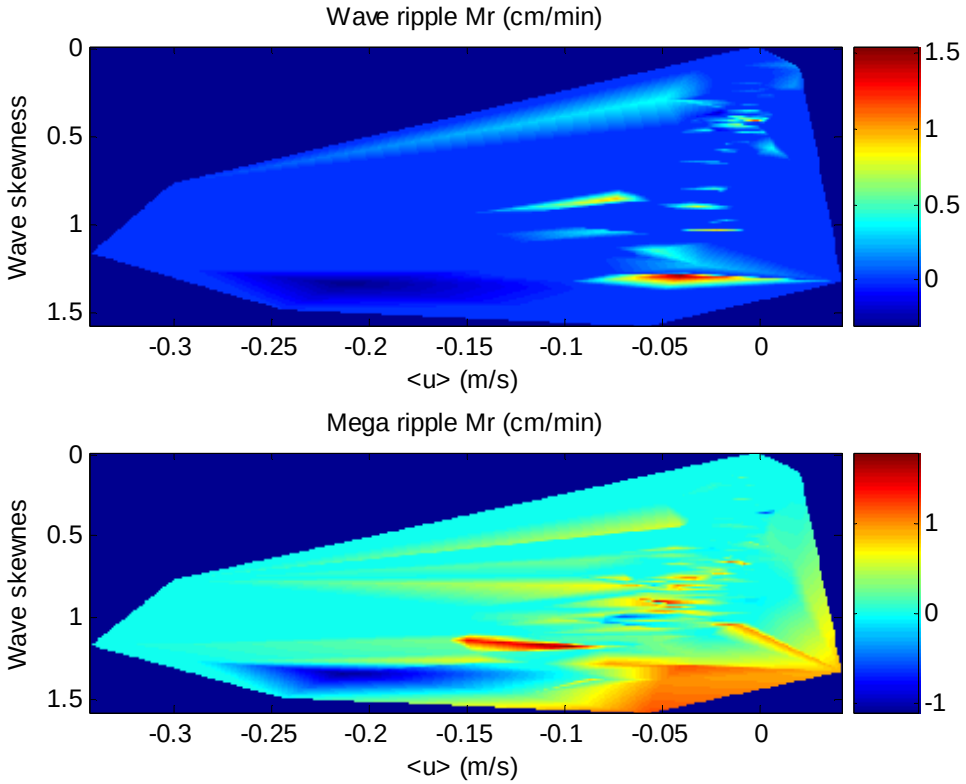

Figure 10: Migration rate (Mr) of wave ripples and megaripples illustrated as a function of wave skewness and mean velocity (<u>).

Conditions in this experiment comprised of both waves and currents, and both wave ripples and megaripples developed (c.f. Blondeaux et al., 2000). As identified by Dyer (1986), one bedform type (ripples) was superimposed on another (megaripples). In this case, these conditions occurred in the lowest wave energy conditions observed (H = 0.46 m), when mean currents were small (<u> < ~0.1 m/s), and when orbital velocity was least (u_m < ~ 0.25 m/s).

10. Conclusion

Wave ripples heights increased with decreasing orbital velocity but reduced in height when mean currents were strong. When developed, wave ripples co-existed with megaripples, and contributed up to 12% of the bed level variance. Megaripples were largest when orbital velocities were in the range 0.25 to 0.4 m/s, and reduced in height with increasing mean current speed. Wave ripple and megaripple migration was generally onshore in deeper water and increased with incident wave skewness in shallower water. However, onshore migration was reduced to zero when the offshore-directed mean flow was greater in magnitude than -0.15 m/s. The persistence of megaripple features through the tide, and the superposition of wave ripples in lower wave energy conditions may be important for bed roughness calculations in nearshore morphological modeling.

Acknowledgements

The fieldwork for this project was funded by a partnership grant from the UK Natural Environment Research Council (NERC) and the UK Royal National Lifeboat Institution (RNLI), 'Dynamics of Rip Currents and Implications for Beach Safety (DRIBS)', (NERC ref: NE/H004262/1).

References

Allen, J.R.L. 1968. *Current ripples: their relation to patterns of water and sediment motion*, North Holland Pub. Co., University of Michigan.

Bagnold, R.A. ,1963. Beach and nearshore processes, in *The Sea*, edited by M.N.Hill, pp 507-553, Wiley Interscience, New York.

Blondeaux, P., Foti, E. & Vittori, G., 2000. Migrating sea ripples. *European Journal of Mechanics - B/Fluids*, 19 (2). 285-301.

Crawford, A.M., and Hay,A.E., 2001. Linear transition ripple migration and wave orbital velocity skewness: Observations, *J. Geophys. Res*, 106, 14,113-14,128.

Davidson, M., Huntley, D., Holman, R., George, K., 1997. The evaluation of Large Scale (km) Intertidal Beach Morphology on a Macrotidal Beach Using Video Images. Proceedings Coastal Dynamics 97. 385-394.

Dyer, K.R., 1986. *Coastal and Estuarine Sediment Dynamics*, Wiley Interscience, Chichester.

Elgar, S., Guza, R.T. and Freilich, M., 1998. Eulerian measurements of horizontal accelerations in shoaling surface gravity waves, *Journal of Geophysical Research*, 93, 9261 9269

Fredsoe, J. & Deigaard, R., 1993. *Mechanics of coastal sediment transport*. Advanced series on ocean engineering. vol. 3. World Scientific. London.

Gallagher, E.L., 2003. A note on megaripples in the surfzone: evidence for their relation to steady flow dunes. *Marine Geology Research Letters*, 193. 171-176.

Gallagher, E.L., Elgar, S., Thornton, E.B., 1998. Megaripple migration in a natural surfzone. *Nature*, 394. 165-168.

Masselink, G. & Black, K.P., 1995. Magnitude and cross-shore distribution of bed return flow on natural beaches. *Coastal Engineering*. 25, 165–190.

Masselink, G. & Hughes, M. G., 2003. *Introduction to Coastal Processes & Geomorphology.* Hodder Education. London.

Masselink, G., Austin, M., O'Hare, T. & Russell, P., 2007. Geometry and dynamics of wave ripples in the nearshore of a coarse sandy beach. *Geophysical Research Letters*, 112.

Miles, J. 2013. Wave shape effects on sediment transport. *Proceedings 12th International Coastal Symposium* (Plymouth, England), *Journal of Coastal Research.* Special Issue No 65.

Nielsen, P., 1992. *Coastal bottom boundary layers and sediment transport.* Advanced series on ocean engineering. World Scientific. London.

Sherman, D. J., Short, A. D. & Takeda, I., 1993. Seiment Mixing-Depth and Bedform Migration in Rip channels. *Journal of Coastal Research*, 15. 39-48.

Thornton, E.B., Swayne, J.L., and Dingler, 1998. Small scale morphology across the surf zone. *Mar Geol 145*, 173-196.

Thorpe, A., Miles, J., Masselink, G., Russell, P., Scott, T., and Austin, M. 2013. Suspended sediment transport in rip currents on a macrotidal beach. *Proceedings 12th International Coastal Symposium* (Plymouth, England), *Journal of Coastal Research.* Special Issue No 65.

Traykovski, P., Hay, A.E., Irish, J.D., and Lynch, J.F., 1999. Geometry, migration, and evolution of wave orbital ripples at LEO-15, *J. Geophys. Res., 104*, 1505-1524.

Vincent, C.E., and Osborne, P.D., 1993. Bedform dimensions and migration rates under shoaling and breaking waves. *Cont. Shelf Res. 13*, 1267-1280.

Yalin, M.S., 1964. On the average velocity of flow over a mobile bed. *La Houille Blanche*, 1. 45-53.